

Retraction

Retracted: Research on Digital Image Watermarking Algorithm Based on Scrambling and Singular Value Decomposition

Journal of Mathematics

Received 19 December 2023; Accepted 19 December 2023; Published 20 December 2023

Copyright © 2023 Journal of Mathematics. This is an open access article distributed under the Creative Commons Attribution License, which permits unrestricted use, distribution, and reproduction in any medium, provided the original work is properly cited.

This article has been retracted by Hindawi following an investigation undertaken by the publisher [1]. This investigation has uncovered evidence of one or more of the following indicators of systematic manipulation of the publication process:

- (1) Discrepancies in scope
- (2) Discrepancies in the description of the research reported
- (3) Discrepancies between the availability of data and the research described
- (4) Inappropriate citations
- (5) Incoherent, meaningless and/or irrelevant content included in the article
- (6) Manipulated or compromised peer review

The presence of these indicators undermines our confidence in the integrity of the article's content and we cannot, therefore, vouch for its reliability. Please note that this notice is intended solely to alert readers that the content of this article is unreliable. We have not investigated whether authors were aware of or involved in the systematic manipulation of the publication process.

Wiley and Hindawi regrets that the usual quality checks did not identify these issues before publication and have since put additional measures in place to safeguard research integrity.

We wish to credit our own Research Integrity and Research Publishing teams and anonymous and named external researchers and research integrity experts for contributing to this investigation.

The corresponding author, as the representative of all authors, has been given the opportunity to register their agreement or disagreement to this retraction. We have kept a record of any response received.

References

- [1] L. Pei, "Research on Digital Image Watermarking Algorithm Based on Scrambling and Singular Value Decomposition," *Journal of Mathematics*, vol. 2022, Article ID 4656010, 10 pages, 2022.

Research Article

Research on Digital Image Watermarking Algorithm Based on Scrambling and Singular Value Decomposition

Lei Pei 

University of Science and Technology Beijing, Beijing 100083, China

Correspondence should be addressed to Lei Pei; peilei@ustb.edu.cn

Received 21 December 2021; Revised 21 January 2022; Accepted 10 February 2022; Published 27 February 2022

Academic Editor: Naeem Jan

Copyright © 2022 Lei Pei. This is an open access article distributed under the Creative Commons Attribution License, which permits unrestricted use, distribution, and reproduction in any medium, provided the original work is properly cited.

At present, the digital image watermarking algorithm has not embedded the synchronization signal in the image, resulting in the poor performance of the embedded image in terms of, for example, imperceptibility, anti-attack ability, and robustness. Therefore, a digital image watermarking algorithm based on scrambling and singular value decomposition is proposed. The digital watermark is preprocessed by dimensionality reduction and encryption; the digital image is processed in sections and embedded in the synchronization signal. The digital watermark image is embedded in the digital image watermark by using the low-frequency energy ratio technology of sound channel. The watermark image extraction step is designed to extract the watermark image. The transmittance of the degraded image is calculated, the transmittance is refined by relying on the soft matting algorithm and guiding filter, the image contrast in the image frequency domain is enhanced, and the results are mapped to the appropriate visual range to optimize the visual brightness of the image. Finally, according to the uniqueness of singular value matrix, the distributed characteristics of image matrix data are described, the visual effect is enhanced, and the research of digital image watermarking algorithm is completed. The experimental results show that the algorithm can extract the watermark information completely, the image contrast and singular value have been significantly improved, and the algorithm has better anti-attack performance.

1. Introduction

With the rapid development of network technology and digital multimedia technology, digital photos, paintings, voice, text, video, and other products have been very common [1]. However, with the development of digital technology and networking [2], fast, accurate, and cheap digital transmission means bring opportunities to countless businesses but also pose new challenges, including infringement, piracy, and arbitrary tampering with digital products (such as electronic publications, audio, video, animation, and image products). This leads to the problems of digital information security and digital product copyright protection. Digital image watermarking technology came into being in this environment [3]. It is regarded as the last line of defense of information security and has attracted extensive attention from all walks of life. Among digital image watermarking techniques, digital image watermarking considering scrambling and singular value

decomposition is the core one. Digital image refers to the display image in two-dimensional digital form, which always takes digital unit as pixel representation structure, which can better describe the mathematical relationship between real image and virtual image [4]. Digital image watermarking algorithm is a process of hiding secret information into the host image to prevent the repeatability of original data and maintain authenticity, subtitle, and copyright control [5, 6].

At present, mankind has entered the digital information age. Through digital media, we can spread and obtain network information such as audio and video, which has greatly enriched people's lives and improved the transmission efficiency of information. Some scholars put forward relevant research. Reference [7] proposed a sparse domain lossless digital image watermarking algorithm based on k-singular value decomposition algorithm and introduced a robust lossless sparse domain watermarking algorithm combined with discrete cosine transform (DCT), which hides secret information into important sparse

elements of the host image. In order to improve the security of the original image, the secret information is first transformed by a discrete cosine transform. These DCT coefficients with some regularization parameters will be inserted into the selected important sparse coefficients. In the extraction stage, the sparse domain orthogonal matching pursuit algorithm is used to extract secret information from important sparse coefficients. Finally, the inverse discrete cosine transform is used to extract secret information without losing any information.

Reference [8] proposed a robust logo watermarking algorithm based on the maximum wavelet transform. Digital image watermarking is used to protect the copyright of digital images. A new blind logo image watermarking technology for RGB images is proposed. This technology makes use of the error correction ability of the human visual system. It embeds two different watermarks in the wavelet/multiwavelet domain. The two watermarks are embedded in different subbands and are orthogonal for different purposes. One is a high-capacity multibit watermark for embedding the logo, and the other is a watermark for detecting and reversing geometric attacks. Both watermarks are embedded using the spread spectrum method, based on pseudorandom noise sequence and unique key. By embedding a watermark into the modulus maxima coefficients of the wavelet transform, the robustness to geometric attacks such as rotation, scaling, and translation is realized. Although the above methods have made some progress, with the development of digital technology, security problems of digital information have been caused, such as copyright infringement, illegal copying of software or documents, and wanton tampering with digital information. Due to the visual quality conditions of digital images, there will be obvious loss of watermark pixels in the spatial domain environment. In order to solve these problems, based on the above research, a digital image watermarking algorithm based on scrambling and singular value decomposition is proposed.

The following is a summary of the research: Section 1 contains the introduction. Section 2 discusses the research on digital image watermarking algorithm. Section 3 discusses the visual effect enhancement of the digital image watermarking algorithm under scrambling and singular value decomposition. Section 4 discusses the experimental analysis with tables. Finally, the conclusion brings the paper to an end in Section 5.

2. Research on Digital Image Watermarking Algorithm

The suggested approach preserves the watermarked image's invisibility and quality. The developed algorithm is a blind watermarking technique that meets invisibility and robustness requirements. A watermark is embedded in the middle-frequency coefficient block of three DWT levels to accomplish watermarking.

2.1. Preprocessing Digital Image Watermarking. In order to make the digital image watermark random before

embedding audio and robust in the process of processing, dimensionality reduction and encryption preprocessing are carried out for the digital image watermark [9]. Select one frame image in the digital image sequence, and obtain three high-frequency bands and one low-frequency band along with the horizontal and vertical directions. The structure is shown in Figure 1.

In Figure 1, the high-frequency part in the horizontal direction and the low-frequency part in the vertical-horizontal direction of the image are represented as BB1; the low-frequency part in the horizontal direction and the high-frequency part in the vertical direction are represented as CC1; and when both the horizontal direction and the vertical direction are high-frequency parts, they are represented as DD1. AA1 retains the main features of the image to be detected, and the other three high-frequency bands maintain the edge details. Assuming that the selected digital image watermark with the size of $S_1 \times S_2$ is S , the pixel amplitude s of the digital image watermark is

$$S = \{s(x, y), \quad 0 \leq x < S_1, 0 \leq y < S_2\}, \quad (1)$$

where $s(x, y)$ represents the pixel amplitude of the digital image watermark at position (x, y) . According to (1), the digital image watermark is preprocessed [10], and the processing process is as follows:

Step 1. Dimensionality reduction. Since digital image signal belongs to one-dimensional signal, dimensionality reduction is carried out for digital image signal [11], and it is transformed into a one-dimensional sequence. Then, the one-dimensional sequence V of digital image watermark image after dimensionality reduction is

$$R = \{r(n) \times s(x, y), \quad n = x \times S_2 + y, n \in S_1 \times S_2\}, \quad (2)$$

where n represents the length of the digital image and $r(n)$ represents the sequence of digital image watermark when the length of the digital image is n .

Step 2. Watermark image encryption. The digital image watermark sequence obtained by scrambling formula (2) needs to use logistic chaotic mapping to generate the binary chaotic sequence. The processing formula is as follows:

$$E = f(n) \times e(n) \oplus l(n), \quad (3)$$

where E represents the scrambled digital image watermark signal, $f(n)$ represents the scrambled digital image watermark signal when the digital image length is n , \oplus represents the algorithm, $e(n)$ represents the one-dimensional sequence of digital image watermark, and $l(n)$ represents the binary chaotic sequence. According to the encrypted digital image watermark image obtained by (3), the digital image watermark is encrypted by using the sensitivity of chaotic sequence to the initial value, and the watermark spectrum has high balance and security [12].

When embedding the visibility watermark in the digital image, in most cases, the visibility watermark should maintain a clear and visible existence state, which is very easy to be found by the human eye. However, since it cannot

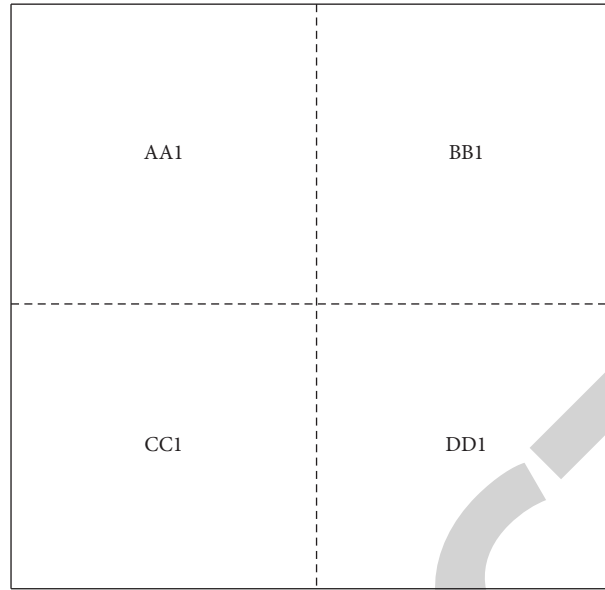


FIGURE 1: Video image structure decomposed by wavelet transform.

affect the original detail characteristics of the digital image, the impact on the quality of the digital image should be kept as small as possible, so as not to be too prominent and attract the attention of the human eye. It can be seen that digital image watermarking does not need to be completely confidential, but it must have a certain representative significance. Based on this, all watermarks in the digital image are counted, and then the embedded synchronous signal processing is implemented for the segmented original image, until the standard information deviation in each block space environment and the real-time display strength of the watermark node are calculated and the research of digital image watermarking algorithm is completed.

2.2. Embedded Synchronization Signal. In this study, the digital image watermarking algorithm is studied. The digital image is segmented, and the length of each signal is the same, which is n . A synchronization signal is hidden in each digital image and embedded in the time domain [13]. At this time, it is also necessary to control the number of synchronization codes to avoid the contradiction between transparency and robustness of the algorithm and reduce the amount of search calculation of the algorithm.

Therefore, it is assumed that the synchronization signal embedded in the time domain is $\{a_n\}$ and $\{a_n\} \in \{-1, 1\}$, where n represents an appropriate threshold and takes an odd number. A total of k digital images are segmented this time, and there are B sampling points in each digital image $A(k)$. When the synchronization signal $b(i)$ is embedded in B_1 , the sampling point B is the B_1 bit of the sampling point, where i represents the i audio data. Then, the digital image $X(u)$ embedded in the synchronization signal is

$$X(u) = \begin{cases} x(u), & \text{mod} \left[\frac{x(u)}{B}, 2 \right] = a(n), \\ x(u) + \frac{m}{2}, & \text{mod} \left[\frac{x(u)}{B}, 2 \right] \neq a(n). \end{cases} \quad (4)$$

In (4), m represents a positive integer, [Brackets value] represents an integer operation, and mod represents the factorial of a positive integer.

According to (4), the synchronization signal is embedded in the digital image. At this time, the watermark can be embedded in the digital image according to the synchronization signal.

2.3. Embedding Digital Image Watermark with Low-Frequency Energy Ratio of Sound Channel. After the digital image watermark image is preprocessed, the synchronization signal is embedded in the digital image. At this time, the digital image watermark can be embedded in the digital image by using the channel low-frequency energy ratio technology [14]. The embedding process is as follows:

- (i) Step 1: Frame processing embeds the original image signal into the sync signal. The digital image signal of the embedded synchronization signal obtained according to formula (4) is $X = \{x(u), 0 \leq u \leq n\}$, and $x(u) \in \{0, 1, 2, \dots, (2^P - 1)\}$ is the amplitude of the u audio data. If the original audio is divided into several lengths, its length is determined by the original image signal and the amount of watermark information to be embedded, that is,

$$X = \left\{ X(q), \quad 0 \leq q \leq \frac{l}{N} \right\}. \quad (5)$$

- (i) In (5), N represents the amount of data contained in each frame signal and l/n represents the number of data segments divided into the whole audio segment.
- (ii) Step 2: Select the embedded frame. According to the segmentation processing steps when embedding the synchronization signal, segment the digital image, mark each segment of the signal, and calculate the audio energy D_v calculation formula of each frame:

$$\begin{cases} D_1 = \sum_{i=0}^{l'=1} x^2(n), \\ D_v = \sum_{i=0}^{n'=1} x^2[(a-1) \times n']. \end{cases} \quad (6)$$

- (i) In (6), F represents the total number of frames of the image signal and D_v represents the audio energy of the v frame. According to (6), calculate the energy of all audio frames and arrange them in descending order. Considering the robustness and imperceptibility of the watermark, the audio frame with large energy is selected and embedded in the digital image. Only 1 bit is embedded in the watermark information of each image signal.
- (ii) Step 3: Calculate the average value W of the selected embedded frame. When $W < 0$, the inverse signal of the embedded frame signal needs to be taken, and then the inverse transform is carried out. When $W > 0$, the complex cepstrum of each frame image signal can be calculated. Therefore, assuming that the f audio data frame of the i frame is $X_f(i)$, the complex cepstrum C_f^i of the image signal of each frame is

$$C_f^i = C_{\text{cceps}}(X_f(i)), \left(1 \leq f \leq \frac{l}{N}, 1 \leq i \leq N\right). \quad (7)$$

- (i) In (7), C_{cceps} represents the number of additional delay samples when the f frame image signal is subjected to complex cepstrum transformation and returns to the audio frame $X_f(i)$.
- (ii) Step 4: Calculate the low-frequency energy of the channel. Assuming that the complex cepstrum coefficient of the j scale factor is C_j , the low-frequency energy E_j of the j scale factor is

$$E_j = \sum_{j=S_{\text{starti}}}^{E_{\text{endi}}} C_f^i. \quad (8)$$

- (i) In (8), E_{endi} represents the end of the j scale factor band index and S_{starti} represents the beginning of the j scale factor band index.
- (ii) Step 5: Quantify the low-frequency energy of the channel. Assuming that the quantization step of channel low-frequency energy is q , the measured channel low-frequency energy E_j is

$$E_j' = \left[\text{round}\left(\frac{E_j}{2q} - \frac{p}{2}\right) \right] \times 2q + pq. \quad (9)$$

- (i) In (9), $\text{roun } d$ represents rounding, and p represents the number of bits used for each data.
- (ii) Step 6: Adjust the complex cepstrum coefficient C_f^i of each frame image signal, and perform inverse cepstrum transform X_f^i ; then,

$$\begin{aligned} C_f^i &= C_f^i + \alpha, \\ X_f^i &= \text{icceps}(C_f^i, d(f)). \end{aligned} \quad (10)$$

- (i) In (10), icceps represents the inverse transform function, α represents the change of the mean value of the complex cepstrum coefficient after quantization, and C_f^i represents the i complex cepstrum coefficient of the f frame.
- (ii) Step 7: Repeat steps 3 to 6 until all watermark information is embedded in the whole digital image signal; that is, the watermark embedding is completed.

2.4. Extracting Digital Image Watermark. According to the digital image watermark embedding process designed in Section 2.3, the digital image watermark is extracted. The watermark image extraction is the calculation link of the design of the new digital image watermark algorithm. With the support of scrambling and singular value decomposition, the actual position of the image information node in the spatial domain environment can be determined, and then through function processing, realize the conversion from clear watermark to fuzzy watermark. In a complete digital image, due to the influence of spatial domain change conditions, the watermark node is basically always in a changing state. In this case, some pixels may be covered by interfering noise, resulting in the continuous decline of the execution ability of the watermark node. To solve this problem, after the visible watermark processing is completed, the position of individual pixel noise should be limited to realize the watermark extraction processing. The extraction process is shown in Figure 2.

According to the watermark extraction process shown in Figure 2, in the watermark embedding process, the frame division process is used to split watermarked image signal into frames and complex cepstral transform and calculate the mean value of complex cepstrum coefficient of each frame image signal. Therefore, assuming that the selected digital image is $X' = \{X'(k), 1 \leq k \leq z\}$, where z represents the number of frames embedded with the digital image watermark, the watermark sequence W_f before inverse scrambling is

$$W_f = \begin{cases} 1, & \text{if } \text{mod}(m'_f, 2) = 1, \\ 0, & \text{if } \text{mod}(m'_f, 2) = 0. \end{cases} \quad (11)$$

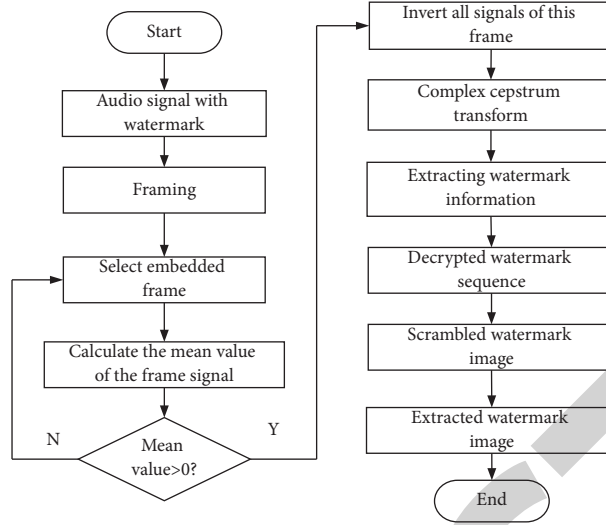


FIGURE 2: Watermark extraction process.

In (11), m_f represents the mean value of the complex cepstrum coefficient of each frame of image signal. Let k_0 represent the pixel extraction coefficient at the initial stage of spatial domain watermark embedding and k_n represent the pixel extraction coefficient at the end of spatial domain watermark embedding. The extraction expression at the watermark node can be defined as

$$Y_U = \frac{1}{A} \sum_{k_0}^{k_n} |K \times z_{\max} - K' \times z_{\min}|. \quad (12)$$

In (12), K and K' represent two different discrete Fourier function transformation conditions, and z_{\min} and z_{\max} represent the minimum and maximum amount of watermark information data in digital image spatial domain, respectively. According to logistic chaotic map, binary chaotic sequence is generated, and the watermark sequence before inverse scrambling is decrypted to obtain one-dimensional sequence; the dimension of one-dimensional sequence is raised to obtain two-dimensional image. The dimension raising process is the inverse process of dimension reduction in watermark image preprocessing, so as to extract digital image watermark.

3. Visual Effect Enhancement of Digital Image Watermarking Algorithm under Scrambling and Singular Value Decomposition

3.1. Digital Image Transmittance Estimation. In the digital image, if the transmittance and atmospheric spectrum can be obtained from the image, the blurred area in the digital image can be restored to normal Z . There are three unknown parameters in the operation formula (13) of digital image, which is an ill-conditioned equation. Some a priori conditions need to be used to operate the ill-conditioned equation. A priori dark color system can solve this problem very well.

$$C_E(x) = Z(x)m(x) + A_z(1 - m(x)). \quad (13)$$

In (13), $C_E(x)$ represents the reflected light intensity of the scene point collected by the observation point, $Z(x)$ represents the pixel in the image, $m(x)$ represents the transmittance of the light area, and A_z represents the atmospheric luminosity.

If the atmospheric light is homogeneous, (13) is satisfied for all channels in the RGB color space. It is proposed that the atmospheric light is known, and it is further proposed that the transmittance is normally bright in local areas. Assuming the transmittance equation $\tilde{m}(x)$ of this region, calculate the dark primary color for (13), and the equation is as follows:

$$U_{ty} = \tilde{m}(x) \min_{y \in \Omega(x)} \frac{Z^c(y)}{A^c} + (1 - \tilde{m}(x)). \quad (14)$$

In (14), $Z^c(y)$ represents the pixel ordinate in the image, A^c represents the local window centered on the abscissa and ordinate, and $\Omega(x)$ represents a color channel in the RGB color space of the image Z . With (14), the dark primary color calculation of the digital image is reduced to tend to 0.

In fact, there are no particles in the atmospheric light in the normal image. When viewing distant objects, the image is still a digital image. Therefore, in this paper, a small number of degraded areas are reserved in a certain area of the ordinary image. By integrating a constant parameter $\omega \in [0, 1]$, the rough transmittance calculation formula is

$$\tilde{m}(x) = 1 - \omega \min_{y \in \Omega(x)} \left(\frac{Z^c(y)}{A^c} \right). \quad (15)$$

In fact, the transmittance is not always the same in a region. For example, when the depth of field protrudes, the transmittance will change.

3.2. Fine Processing of Digital Image Transmittance. Directly processing the blurred area in the digital image through rough transmittance will lead to obvious halo in the

background of the image. In order to remove the halo effect, the transmittance is refined by soft matting algorithm and guided filter.

3.2.1. Soft Matting Algorithm. The soft matting formula is as follows:

$$I_o = \alpha_1 \times Q_1 + (1 - \alpha_1)B_n. \quad (16)$$

In (16), Q_1 represents the foreground, B_n represents the background, α_1 represents the image, and I_o represents the image fused by the foreground and the background. Through the above calculation, it is found that the transmittance distribution is affected by the corresponding soft matting formula. To refine the transmittance, the soft matting algorithm can obtain better-refined transmittance.

3.2.2. Guided Filter. The guided filter is an edge-preserving smoothing filter, which has a good effect on smoothing filtering and edge-preserving. If the output degraded image formula q_1 , the guidance diagram formula I_i , and the input digital image formula p_1 are proposed, there is a linear correlation between the output image and the guidance diagram in the local window w_{k1} . The guidance filter equation is as follows:

$$D_q = (a_{k1}I_i + b_{k1}) + (q_1 \times p_1 \times w_{k1}). \quad (17)$$

In (17), a_{k1} and b_{k1} are linear constant coefficients of local window w_{k1} . By calculating the linear constant coefficient, the difference between the input images is minimized, and it is proved that the edge of the guide image and the output image can be consistent. Since the guided filter can only be calculated by matrix point multiplication and mean filtering, it can be optimized through the integral image algorithm, so that the guided filter is only associated with the image size N and is not associated with the window size. Then, the time complexity of the guided filter is $O(N)$. Relying on the guided filter can effectively improve the calculation efficiency of the soft matting algorithm.

3.3. Digital Image Visual Effect Enhancement

3.3.1. Frequency Domain Enhancement. In digital images, the movement of pixel gray value will be represented by frequency. Frequency description is a spatial frequency that changes with the change of coordinates. For the characteristics of lines, noise, and edges, such as lakes, rivers, or roads with large differences, there are large spatial frequencies. The frequency domain is a stable structure with large gray value change frequency and large area in a short pixel size.

Frequency enhancement is to calculate the Fourier transform coefficient in the frequency domain of the digital image and then change it back to the initial spatial domain to obtain the image with enhanced details. Frequency domain enhancement is an indirect processing method. Firstly, the digital image is processed by Fourier transform, and the frequency domain of the image is filtered. Finally, the low-

frequency part of the image is transformed into a more stable region. Specifically, it has the characteristics of high pass, low pass, and homomorphic filtering and band stop in the frequency domain.

Frequency domain enhancement has three processes, namely:

- (1) Transferring the digital image in the spatial domain to the frequency domain.
- (2) Enhancing the image in the frequency domain [4].
- (3) Returning the enhanced image in the frequency domain to the spatial domain.

If the convolution of linear bit invariant operator $h(x, y)$ and function $f(x, y)$ is $g(x, y)$, that is, $f(x, y) = h(x, y) \otimes g(x, y)$, then it exists in the frequency domain by virtue of the convolution theorem:

$$G(u, v) = H(u, v)F(u, v). \quad (18)$$

In (18), $G(u, v)$, $H(u, v)$, $F(u, v)$ represent the Boyle transformation of $G(x, y)$, $H(x, y)$, $F(x, y)$, respectively, and $H(u, v)$ can be described as a transfer function through the linear coefficient theory.

$f(x, y)$ is the set input image, and $H(u, v)$ needs to be determined. After determining $H(u, v)$, $g(x, y)$ with required characteristics can be obtained after calculating $G(u, v)$ by

$$g(x, y) = T^{-1}[H(u, v)F(u, v)]. \quad (19)$$

In (19), T^{-1} represents the required time transpose. With the above calculation, the frequency domain of the digital image can be enhanced, so as to improve the contrast details in the image.

3.3.2. Brightness Intensity Component Enhancement. The pixel brightness intensity on both sides of the inner edge of the digital image is quite different from that at the center of the image. Therefore, if you want to enhance the image, you need to compare the pixels in the image one by one, and the brightness intensity value is regarded as the external stimulus. Then, the pixel set close to the space and with the same intensity can be expressed as synchronous ignition, and vice versa. This can be expressed in image visual enhancement: synchronous ignition means that there is the same brightness intensity between pixels, and the image area can be smoothed through brightness. Asynchronous ignition means that pixels produce different brightness intensities. Relying on the same and different ignition, we can improve the brightness gradient between image areas, so as to highlight the edge of the digital image, so as to improve the image brightness intensity distribution and make the image have a more obvious hierarchy.

Because the brightness range of the digital image is small, the image contrast decreases. If human visual characteristics are added to the image contrast enhancement algorithm, the contrast enhancement effect can be effectively improved. This is because the brightness perceived by the human visual system has a logarithmic relationship with the brightness that can be obtained by the personnel, so the image contrast within the personnel's visual range can be greatly improved.

In digital image, due to the effect of hard limiting function, the output digital image will be transformed into binary image. In order to enable the output mapping function to effectively enhance the brightness of the image, the brightness intensity of the image is mapped within a suitable visual range by using the logarithmic mapping function according to the human visual characteristics. The calculation formula is as follows:

$$Y_{ij}(n) = 1nI_{\max} - \frac{\Delta t}{\tau_{\theta}}(n-1). \quad (20)$$

In (20), I_{\max} represents the intensity value of the brightest pixel in the initial image; n represents the ignition time $n = 1, 2, 3$; $\Delta t/\tau_{\theta}(n-1)$ represents the attenuation step of the dynamic threshold function in the image at the $(n-1)$ ignition time; and $Y_{ij}(n)$ represents the perceived output at the ignition time, that is, the brightness intensity of the enhanced digital image.

3.3.3. Singular Value Decomposition. Digital image can be represented as a matrix composed of multiple nonnegative scalars. This matrix has the unique characteristic of singular value, which can describe the distribution characteristics of matrix data. It is very stable to describe the image by singular value, and it also has the characteristics of transpose, image invariance, translation, and rotation. It can effectively describe the algebraic features in the image. Therefore, the purpose of enhancing the image can be achieved by enhancing the singular value of the image matrix.

The singular value of the matrix can be obtained by singular value decomposition. The definition of singular value decomposition is as follows: A is proposed to represent $m \times n$ real matrix, and $\text{rank}(A) = r$; then, there are m order West matrix U and E order West matrix V , so that

$$A = USV^H \times U \sum V^H, U * U^H. \quad (21)$$

In (21), V^H represents all r nonzero singular values of A ; each column of U and V is the eigenvector of $A * A^H$ or $A^H * A$, respectively; and S represents the decomposed singular value matrix.

After singular value decomposition, the set information and texture of the image will appear in the matrix U, V , and the energy information of the image will be concentrated in the singular value. The singular value of the image matrix is enhanced by incorporating a certain amount of Gaussian noise into the image. The general process is as follows:

- (1) The preprocessed image $f(x, y)$ is subjected to singular value decomposition to obtain the matrix U, S, V .
- (2) The Gaussian noise is superimposed into the preprocessed image, and the noisy image is decomposed by singular value decomposition to obtain matrix U_n, S_n, V_n .
- (3) The image enhanced by singular value decomposition is $g(x, y) = US_nV_n^H$; $g(x, y) = US_nV_n^H$.

- (4) The image $f(x, y)$ is modified by the adaptive histogram averaging method to obtain the final visual effect enhanced image, so as to complete the research on the digital image watermarking algorithm based on scrambling and singular value decomposition.

4. Experimental Analysis

With the support of scrambling and singular value decomposition, the effect and feasibility of the designed digital image watermarking algorithm are verified. Therefore, a simulation experiment is designed for verification. The MATLAB programming parameters required for the specific experiment are shown in Table 1.

Set the digital image watermark embedding intensity coefficient as 0.1 according to the parameters in Table 1, and draw the waveform of the original image signal and the watermark image signal embedded by the digital image watermark algorithm based on scrambling and singular value decomposition. The experimental results are shown in Figure 3.

According to Figure 3, after introducing the digital image watermarking algorithm based on scrambling and singular value decomposition studied in this paper, there is almost no difference between the waveform of the watermarked image signal and the original signal. It can be seen that there is no obvious difference between them in the process of watermark inspection and testing. According to the above analysis, when the image is not attacked, the watermark information can be completely extracted.

The normalized correlation coefficient (NC) mainly describes the robustness of the watermark. The main factors affecting the robustness of the watermark are various attacks. Select the original image as the test object, and count the normalized correlation coefficient values of the three video watermarking algorithms after various attacks. Suppose that the sampling point of the audio is o , the total length of the audio is L , the original carrier audio is X , and the embedded watermark audio is X' ; then, the normalized correlation coefficient calculation formula S of watermark audio is

$$S = 10 \log_{10} \frac{\sum_{i=0}^L X^2(i)}{\sum_{i=0}^L [X(i) - X'(i)]^2}. \quad (22)$$

Calculate the normalized correlation coefficient results according to (13), as shown in Table 2.

As can be seen from Table 2, compared with the algorithms in [7] and [8], the normalized correlation coefficient of the algorithm in this paper is larger, indicating that the detected watermark is more similar to the original watermark, and the watermark has strong robustness and can resist various attacks. This is mainly because the algorithm in this paper considers scrambling and singular value decomposition, and the watermark is more robust.

In order to further prove the practicability of the proposed method, six digital images are extracted from the image database, and the singular values and contrast increments of the six digital images before and after enhancement are compared. The results are shown in Table 3.

TABLE 1: MATLAB programming parameters.

Programming tools	Algorithm interpretation	Programming tools	Algorithm interpretation
MATLAB main toolbox	Main toolbox required by MATLAB	Communication toolbox	Watermark information toolbox
System identification toolbox	Discrete Fourier transform tool	Fuzzy logic toolbox	Multiresolution decomposition tool
Signal processing toolbox	Programming signal processing tools	Spline toolbox	Digital image spline processing tool

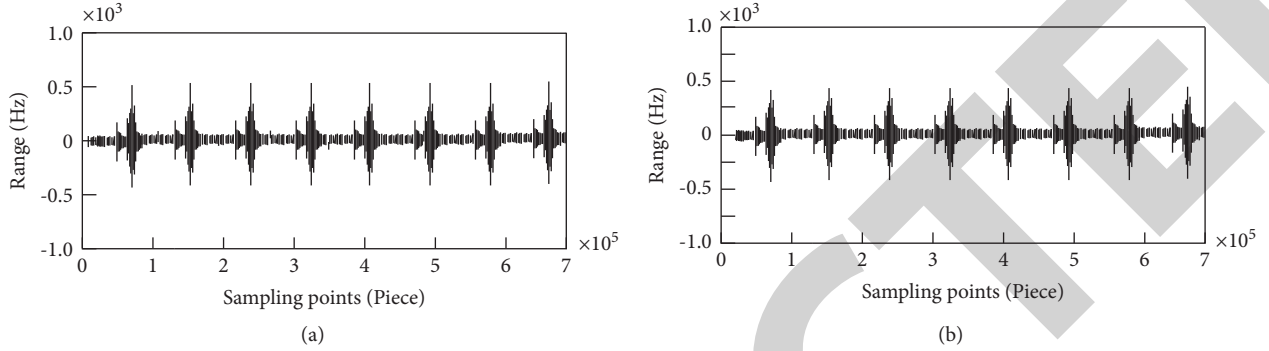


FIGURE 3: Amplitude value of image signal.

TABLE 2: Comparison results of normalized correlation coefficients of different algorithms.

Aggressive behavior	Paper algorithm	Reference [7] algorithm	Reference [8] algorithm
Noise	0.972	0.825	0.937
Frame loss	0.963	0.867	0.920
Shear	0.946	0.838	0.902
Tampering	0.955	0.857	0.910
Compression	0.955	0.822	0.910

It can be seen from Table 3 that the image contrast and singular value have been significantly improved after enhancement using the algorithm in this paper. This is because the proposed method will describe the image by singular value, and because of the characteristics of singular value, the improvement of singular value can also drive the improvement of image visual effect.

From the five audio digital images selected in this experiment, the popular audio is selected as the experimental object. Through the correlation coefficient, the resistance of the three groups of algorithms to attacks is verified. The closer the correlation coefficient of the algorithm to 1, the higher the similarity between the extracted watermark information and the original watermark, and the better the anti-attack ability of the algorithm. Therefore, assuming that the original watermark is w , the extracted watermark is w' , the pixel at a certain position of the watermark is (i, j) , and the number of pixels of the watermark is $m * n$, the correlation coefficient C of the algorithm is calculated as follows:

$$C(w, w') = \frac{\sum_{i=1}^m \sum_{j=1}^n w(i, j)w'(i, j)}{\sqrt{\sum_{i=1}^m \sum_{j=1}^n w^2(i, j)} \sqrt{\sum_{i=1}^m \sum_{j=1}^n w'^2(i, j)}} \quad (23)$$

MATLAB software is selected to attack the three algorithms selected in this experiment. Formula (23) is used to calculate the correlation coefficients of the three algorithms and verify the resistance of the three algorithms to attacks, and the experimental results are shown in Table 4.

TABLE 3: Contrast and entropy increment of images before and after enhancement.

Image ↓	Initial digital image		Enhanced digital image	
	Singular value	Contrast ratio	Singular value	Contrast ratio
1	5.55	1.07	5.97	1.24
2	5.43	1.11	5.69	1.22
3	5.35	1.14	5.93	1.24
4	6.80	1.13	7.39	1.27
5	6.81	1.10	7.42	1.27
6	6.90	1.15	7.53	1.28

It can be seen from Table 4 that under the attack of the attack mode set in this experiment, there is a gap of 0.17 and 0.16 between the correlation coefficient of the algorithm in [7] and the algorithm in [8] and the non-attack, respectively, indicating that the similarity between the watermark information extracted by the two groups of algorithms and the original watermark is low, and the anti-attack performance is poor when attacked. Under the attack of the attack mode set in this experiment, there is only a gap of 0.02 between the correlation coefficient and the non-attack. It can be seen that the digital image watermarking algorithm based on scrambling and singular value decomposition in this research has high similarity between the extracted watermark information and the original watermark and has better anti-attack ability when attacked.

TABLE 4: Test results of resistance to attack.

Attack type ↓	Paper algorithm	Reference [7] algorithm	Reference [8] algorithm
Not attacked	1	1	1
MP3 compression	0.89	0.83	0.77
Random shear	0.98	0.82	0.84
Low pass filtering	0.99	0.83	0.73
Downsampling attack	1	0.90	0.85
Adding Gaussian white noise	0.99	0.72	0.91
Denosing attack	1	0.80	0.80
Gravimetric	0.98	0.84	0.81
Upsampling attack	0.99	0.73	0.85
Mean value	0.98	0.83	0.84

5. Conclusion and Prospect

5.1. Conclusion.

- (1) After introducing the digital image watermarking algorithm based on scrambling and singular value decomposition, there is almost no difference between the waveform of the watermarked image signal and the original signal. When the image is not attacked, the watermark information can be extracted completely.
- (2) The watermark detected by this algorithm is more similar to the original watermark. The watermark has strong robustness and can resist various attacks.
- (3) After using this algorithm for enhancement, the image contrast and singular value have been significantly improved.
- (4) The digital image watermarking algorithm based on scrambling and singular value decomposition in this study has high similarity between the extracted watermark information and the original watermark and has better anti-attack ability when attacked.

5.2. *Prospect.* Digital image watermarking algorithm has been fully studied and developed. In the future research work, digital image watermarking technology needs to be deeply studied in the following aspects:

- (1) Research on the robustness, security, and anti-attack ability of the existing digital watermarking algorithms, combined with the digital signal processing technology, will be conducted to find out the relationship between them, so as to find the digital image watermarking technology with better performance.
- (2) Digital watermarking technology based on biometrics can also embed some human characteristics, such as fingerprint, palm print, and other information in the image as copyright authentication, so it may become the focus of research in the future.
- (3) At present, other digital image watermarking technologies can be used as a research direction of digital image watermarking algorithm in the future, such as digital watermarking technology based on graphics, vector graphics, and animation; watermark

embedding algorithm based on triangular patch geometry; audio watermarking algorithm; and video watermarking algorithm.

Data Availability

The data used to support the findings of this study are available from the author upon request.

Conflicts of Interest

The author declares that he has no conflicts of interest.

Acknowledgments

This project was supported by (1) the Social Science Fund of the Ministry of Education of China in 2019, Research on User Experience Design Method of VR Movie Space, Grant no. 19YJC760078, and (2) the State Scholarship Fund for Visiting Scholar of China Scholarship Council in 2019, Grant no. 201906465002.

References

- [1] L. Zhou, J. Rodrigues, W. H. M. M., and L. Vcm, "5G multimedia communications: theory, technology, and application," *IEEE MultiMedia*, vol. 26, no. 1, pp. 8-9, 2019.
- [2] C. D. Mukhopadhyay, P. Sharma, K. Sinha, and K. Rajarshi, "Recent trends in analytical and digital techniques for the detection of the SARS-Cov-2," *Biophysical Chemistry*, vol. 270, no. 1, Article ID 106538, 2020.
- [3] C. Zxab, C. Xwab, C. Cwb, C. Bmb, H. Zd, and Qi. Labc, "Novel quaternion polar complex exponential transform and its application in color image zero-watermarking - Science-Direct," *Digital Signal Processing*, vol. 116, no. 9, Article ID 103130, 2021.
- [4] H. L. Wei and J. X. Wang, "Simulation research on edge sharpening enhancement of motion blurred digital image," *Computer Simulation*, vol. 37, no. 7, pp. 459-462, Article ID 497, 2020.
- [5] W. W. Hu, R. G. Zhou, and Y. C. Li, "Quantum watermarking based on neighbor mean interpolation and LSB steganography algorithms," *International Journal of Theoretical Physics*, vol. 58, no. 1, pp. 1-24, 2019.
- [6] T. Zhu, W. Qu, and W. Cao, "An optimized image watermarking algorithm based on SVD and IWT," *The Journal of Supercomputing*, vol. 25, no. 5, pp. 1-7, 2021.

- [7] F. Deeba, K. She, F. A. Dharejo, and Y. Zhou, "Lossless digital image watermarking in sparse domain by using K-singular value decomposition algorithm," *IET Image Processing*, vol. 14, no. 6, pp. 1005–1014, 2020.
- [8] M. Barr and C. Serdean, "Wavelet transform modulus maxima based robust logo watermarking," *IET Image Processing*, vol. 14, no. 4, pp. 1–8, 2019.
- [9] K. Mun and C. Son, "Design of optimal blind watermarking technique based on MOEA/D," *IET Image Processing*, vol. 14, no. 16, pp. 4368–4375, 2020.
- [10] R. Uppal, "Quantum and dual-tree complex wavelet transform-based image watermarking," *International Journal of Modern Physics B*, vol. 34, no. 04, Article ID 2050009, 2020.
- [11] H. Wei, B. Huo, X. Shao, and X. He, "Digital image correlation with reduced bias error based on digital signal upsampling theory," *Applied Optics*, vol. 58, no. 15, Article ID 3962, 2019.
- [12] K. A. K. Patro and B. Acharya, "An efficient dual-layer cross-coupled chaotic map security-based multi-image encryption system," *Nonlinear Dynamics*, vol. 104, no. 3, pp. 2759–2805, 2021.
- [13] V. Monga, Y. Li, and Y. C. Eldar, "Algorithm unrolling: interpretable, efficient deep learning for signal and image processing," *IEEE Signal Processing Magazine*, vol. 38, no. 2, pp. 18–44, 2021.
- [14] A. Ad, B. My, B. Oeo, B. Hk, A. Ms, and B. HQ, "Stable computation of higher order Charlier moments for signal and image reconstruction," *Information Sciences*, vol. 521, no. 6, pp. 251–276, 2020.